Coherent and incoherent diffractive hadron production in pA collisions and gluon saturation

Kirill Tuchin[1,2]
[1]*Department of Physics and Astronomy, Iowa State University, Ames, Iowa 50011, USA*
[2]*RIKEN BNL Research Center, Upton, New York 11973-5000, USA*
(Received 24 December 2008; published 28 May 2009)

We study coherent and incoherent diffractive hadron production in high-energy quarkonium–heavy nucleus collisions as a probe of the gluon saturation regime of quantum chromodynamics. Taking this process as a model for pA collisions, we argue that the coherent diffractive gluon production, in which the target nucleus stays intact, exhibits a remarkable sensitivity to the energy, rapidity, and atomic number dependence. The incoherent diffractive gluon production is less sensitive to the details of the low-x dynamics but can serve as a probe of fluctuations in the color glass condensate. As a quantitative measure of the nuclear effects on diffractive hadron production we introduce a new observable—the diffractive nuclear modification factor. We discuss possible signatures of gluon saturation in diffractive gluon production at the Relativistic Heavy Ion Collider, the Large Hadron Collider, and Electron Ion Collider.

DOI: 10.1103/PhysRevC.79.055206 PACS number(s): 24.85.+p, 25.40.Ve, 25.75.Dw

I. INTRODUCTION

Coherent diffractive hadron production in pA collisions is a process $p + A \to X + h + [\mathrm{LRG}] + A$, where [LRG] stands for large rapidity gap. We have recently argued in Refs. [1–3] that the coherent diffractive hadron production can serve as a sensitive probe of the low-x dynamics of the nuclear matter. The coherent diffractive production exhibits a much stronger dependence on energy and atomic number than the corresponding inclusive process. Indeed, the diffractive amplitude is proportional to the square of the inelastic one. At *asymptotically* high energies the coherent diffractive events are expected to constitute a half of the total cross section, with other half being all inelastic processes. Therefore, coherent diffraction is a powerful tool for studying the low-x dynamics of quantum chromodynamics (QCD). In particular, we advocated using the coherent diffraction as a tool for studying the gluon saturation [4,5].

The low-x region of QCD is characterized by strong gluon fields [6,7] and can be described in the framework of the color glass condensate [8–13]. Equations describing the color glass condensate take the simplest form in the the mean-field approximation. It is valid for a color field of a heavy nucleus in the multicolor limit; the relevant resumation parameter is $\alpha_s^2 A^{1/3} \sim 1$. To the leading order in this parameter, the nuclear color field is a coherent non-Abelian superposition of the color fields of single nucleons. Higher-order corrections arise due to the nucleon–nucleon or parton-parton correlations within a nucleon. The later contribute toward the gluon saturation in proton.

In all phenomenological applications of the CGC formalism, one usually relies on the mean-field approximations in which only the lowest-order Green's functions are relevant. If rapidity interval $Y = \ln(1/x)$ is such that $\alpha_s Y < 1$, then the low-x quantum evolution effects are suppressed and the color field can be treated quasiclassically. When $\alpha_s Y \sim 1$, the quantum corrections become important and are taken into account by Balitsky-Kovchegov equation [8,14], which is the first (truncated) equation in the infinite hierarchy of the coupled integrodifferential equations governing evolution of Green's functions of all orders (JIMWLK equations [8–13]).

Although corrections to the mean-field approximation, i.e., quantum fluctuations about the classical solution, are assumed to be small in pA collisions at the Relativistic Heavy Ion Collider (RHIC) their detailed phenomenological study is absent. In this article we fill this gap by calculating the differential cross section for the incoherent diffractive gluon production that happens to be proportional to the dispersion of the quasiclassical scattering amplitude in the impact parameter space, as is expected in the Glauber theory [15]. The incoherent diffractive gluon production in pA collisions is a process

$$p + A \to X + h + [\mathrm{LRG}] + A^*, \tag{1}$$

where A^* denotes the excited nucleus that subsequently decays into a system of colorless protons, neutrons, and nuclei debris.

Note, that the incoherent diffraction (1) measures fluctuations of the nuclear color field. At higher energies the color field of protons also saturates. The mean-field approximation is not at all applicable in this case. A quantum fluctuations (e.g., the so-called pomeron loops [16–19]) may be the driving force of the gluon saturation in protons. This problem is of great theoretical and phenomenological interest. However, in spite of considerable theoretical efforts solution to this problem is still illusive (see Ref. [20] for a brief review of recent advances).

Motivated by theoretical and phenomenological interest to the incoherent diffraction as a measure of fluctuations of the saturated nuclear color field, we derive a formula for the incoherent diffractive hadron production (1) in the framework of the color glass condensate using the dipole model of Mueller [21] and use it for numerical study in the RHIC and Large Hadron Collider (LHC) kinematic regions. The limiting cases of large and small invariant masses of the diffractively produced system were previously considered by many authors [22–29]. Inclusion of the diffractive gluon production was recently shown to be essential for the phenomenology of diffractive DIS off heavy nuclei [30]. We generalize there

results for all invariant masses [satisfying Eq. (31)] and include the gluon evolution effects at *all* rapidity intervals. Unlike models based on the leading twist nuclear shadowing [31,32], we explicitly take into account the gluon saturation effects in the nucleus.

The article is structured as following. In Sec. II we review the Glauber approach [15] to the coherent and incoherent diffraction in pA collisions. In Sec. III we discuss generalization of this approached to the case of quarkonium–nucleus scattering in high-energy QCD. We then turn in Sec. IV to the main subject of the article—the diffractive hadron production—and calculate contributions from coherent and incoherent channels in the quasiclassical approximation neglecting the low-x evolution effects. The low-x evolution effects are taken into account in Sec. V.

Numerical results of the diffractive cross section are presented in Sec. VI. Our phenomenological analyses indicates that the kinematic regions of RHIC and LHC are *not* asymptotic as far as the energy dependence of the diffractive hadron production is concerned. We observed that the ratio of the coherent and incoherent diffractive hadron production at midrapidity in pA collisions increases from RHIC to LHC. This is because gluon saturation effects in protons are assumed to be small. Absence of this feature in experimental measurements can serve as an evidence for the onset of gluon saturation in protons.

It is important to emphasize that all our results are obtained without imposing any experimental constraints on the forward-scattering angle measurements. Coherent diffraction measurements require much better forward-scattering angle resolution than the incoherent ones. Therefore, incoherent diffraction may well turn out to be the only one accessible in experiment. We summarize in Sec. VII.

II. DIFFRACTION IN THE GLAUBER MODEL

A. Total cross section for coherent diffraction in pA

A general approach to multiple scattering in high-energy nuclear physics was suggested by Glauber [15]. First, consider the pp scattering and introduce the elastic pp scattering amplitude $i\Gamma^{pp}(s,\mathbf{b})$, where s is the center-of-mass energy squared and $\mathbf{b}$ is an impact parameter. At high energies $\mathbf{b}$ is a two-dimensional vector in the transverse plane. According to the optical theorem,

$$\sigma_{\rm tot}^{pp} = 2\int d^2b\,{\rm Re}\,\Gamma^{pp}(s,\mathbf{b}). \tag{2}$$

The scattering amplitude $\Gamma^{pp}(s,\mathbf{b})$ can be written as

$$\Gamma^{pp}(s,\mathbf{b}) = 1 - e^{-i\chi^{pp}(s,\mathbf{b})}, \tag{3}$$

where $\chi^{pp}(s,\mathbf{b})$ is a change of phase due to interaction at point $\mathbf{b}$. In the following we will always assume the isotopic invariance of the scattering amplitudes, e.g., $\Gamma^{pp}(s,\mathbf{b}) = \Gamma^{pN}(s,\mathbf{b})$, where N stands for a nucleon.

In pA collisions momenta of nucleons can be neglected as compared to the incoming proton momentum. Therefore, their positions $\mathbf{b}_a$, $a = 1,\ldots,A$ are fixed during the interaction. If scattering of proton on a different nucleons is independent, then the corresponding phase shifts $\chi_a^{pN}(s,\mathbf{B}-\mathbf{b}_a)$ add up:

$$\chi^{pA}(s,\mathbf{B},\{\mathbf{b}_a\}) = \sum_{a=1}^{A}\chi_a^{pN}(s,\mathbf{B}-\mathbf{b}_a), \tag{4}$$

where $\mathbf{B}$ is proton's impact parameter. Indeed, this result holds in QCD as was demonstrated by A. Mueller [33], see Sec. III. The scattering amplitude of proton p on a nucleus A reads

$$\Gamma^{pA}(s,\mathbf{B},\{\mathbf{b}_a\}) = 1 - e^{-i\chi^{pA}(s,\mathbf{B},\{\mathbf{b}_a\})} = 1 - \prod_{a=1}^{A} e^{-i\chi_a^{pN}(s,\mathbf{B}-\mathbf{b}_a)}$$
$$= 1 - \prod_{a=1}^{A}[1-\Gamma^{pN}(s,\mathbf{B}-\mathbf{b}_a)]. \tag{5}$$

Introduce the nucleus-averaged amplitude

$$\Gamma_{if}^{pA}(s,\mathbf{B}) = \langle A_i|\Gamma^{pA}(s,\mathbf{B},\{\mathbf{b}_a\})|A_f\rangle, \tag{6}$$

with $|A_i\rangle$ being the initial and $|A_f\rangle$ the final nucleus state. Then, by the optical theorem, the total pA cross section is given by

$$\sigma_{\rm tot}^{pA} = 2\int d^2b\,{\rm Re}\Gamma_{ii}^{pA}(s,\mathbf{b}). \tag{7}$$

Because we neglect motion of nucleons during the interaction, the distribution of nucleons in the nucleus is completely specified by the thickness function $T(\mathbf{b})$:

$$T(\mathbf{b}) = \int_{-\infty}^{\infty} dz\rho_A(\mathbf{b},z), \tag{8}$$

where $\rho_A(\mathbf{b},z)$ is nuclear density and z is the longitudinal coordinate. The thickness function is often written in terms of the mean density of nucleons $\rho = A/(\frac{4}{3}\pi R_A^3)$ and the nuclear profile function $T_A(\mathbf{b})$ as

$$T(\mathbf{b}) = \rho\, T_A(\mathbf{b}). \tag{9}$$

It is normalized as

$$\int d^2b\,T(\mathbf{b}) = \int d^2b\,\rho T_A(\mathbf{b}) = A. \tag{10}$$

Using these definitions we write the diagonal element of Eq. (6) as

$$\Gamma_{ii}^{pA}(s,\mathbf{B}) = \frac{1}{A}\int\prod_{a=1}^{A} d^2b_a\rho T_A(\mathbf{b}_a)\Gamma^{pA}(s,\mathbf{B}-\mathbf{b}_a)$$
$$= 1 - \left[1 - \frac{1}{A}\int d^2b_a\Gamma^{pN}(s,\mathbf{b}_a)\rho T_A(\mathbf{B}-\mathbf{b}_a)\right]^A$$
$$\approx 1 - e^{-\int d^2b_a\Gamma^{pN}(s,\mathbf{b}_a)\rho T_A(\mathbf{B}-\mathbf{b}_a)}, \tag{11}$$

where we assumed that $A \gg 1$.

Impact parameter dependence of the pp collisions is usually parameterized as

$$\Gamma^{pp}(s,\mathbf{b}) = \tfrac{1}{2}\sigma_{\rm tot}^{pp}(s)\,S_p(\mathbf{b}), \tag{12}$$

where we neglected a small imaginary part of $\Gamma^{pp}(s,\mathbf{b})$ and introduced the proton profile function $S_p(\mathbf{b})$ as

$$S_p(\mathbf{b}) = \frac{1}{\pi R_p^2} e^{-\frac{b^2}{R_p^2}}. \tag{13}$$

Phenomenologically, $R_p = \sqrt{2B} \approx 1$ fm, where $B = 12.6\ \mathrm{GeV}^{-1}$. Because the proton radius R_p is much smaller than the radius of a heavy nucleus R_A, we can approximate the proton profile function by the delta function in which case the overlap integral appearing in Eq. (11) becomes simply the nuclear thickness function

$$\int d^2b S_p(\mathbf{b})\, \rho T_A(\mathbf{B}-\mathbf{b}) \approx \rho T_A(\mathbf{B}). \tag{14}$$

This approximation holds when $R_p \ll R_A$, i.e., $A^{1/3} \gg 1$. Actually, this condition follows from a requirement that the quasiclassical approximation holds. Indeed, in the quasiclassical approximation $\alpha_s \ll 1$ and $\alpha_s^2 A^{1/3} \sim 1$ implying that $A^{1/3} \gg 1$.

Using Eqs. (12) and (14) in Eq. (11) we derive

$$\Gamma_{ii}^{pA}(s,\mathbf{b}) = 1 - e^{-\frac{1}{2}\sigma_{\mathrm{tot}}^{pN}(s)\rho T_A(\mathbf{b})}. \tag{15}$$

The cross section of coherent diffraction is given by the elastic cross section

$$\begin{aligned}\sigma_{\mathrm{CD}}^{pA}(s) &= \int d^2b \left|\Gamma_{ii}^{pA}(s,\mathbf{b})\right|^2 \\ &= \int d^2b \left[1 - e^{-\frac{1}{2}\sigma_{\mathrm{tot}}^{pN}(s)\rho T_A(\mathbf{b})}\right]^2.\end{aligned} \tag{16}$$

B. Total cross section for incoherent diffraction in pA

Consider incoherent diffraction of proton p on a nucleus A. In this processes the nucleus gets excited from the initial state $|A_i\rangle$ to any colorless final state $|A_f\rangle$. It may then decay, but it is essential that its constituent nucleons remain intact as color objects. The corresponding cross section reads

$$\begin{aligned}\sigma_{\mathrm{ID}}^{pA}(s) &= \int d^2B \sum_{i\neq f} \langle A_f|\Gamma^{pA}(s,\mathbf{B},\{\mathbf{b}_a\})|A_i\rangle^\dagger \\ &\quad\times \langle A_f|\Gamma^{pA}(s,\mathbf{B},\{\mathbf{b}_a\})|A_i\rangle \\ &= \int d^2B \sum_{f} \langle A_f|\Gamma^{pA}(s,\mathbf{B},\{\mathbf{b}_a\})|A_i\rangle^\dagger \\ &\quad\times \langle A_f|\Gamma^{pA}(s,\mathbf{B},\{\mathbf{b}_a\})|A_i\rangle \\ &\quad - \int d^2B |\langle A_i|\Gamma^{pA}(s,\mathbf{B},\{\mathbf{b}_a\})|A_i\rangle|^2 \\ &= \int d^2B [\langle A_i||\Gamma^{pA}(s,\mathbf{B},\{\mathbf{b}_a\})|^2|A_i\rangle \\ &\quad - |\langle A_i|\Gamma^{pA}(s,\mathbf{B},\{\mathbf{b}_a\})|A_i\rangle|^2],\end{aligned} \tag{17}$$

where in the last line we used the completeness of the set of nuclear states. We arrived at the well-known result that the cross section for the incoherent diffraction at a given impact parameter $\mathbf{B}$ is given by the square of the standard deviation of the scattering amplitude $\Gamma^{pA}(s,\mathbf{B},\{\mathbf{b}_a\})$ from its mean-field value $\langle A_i|\Gamma^{pA}(s,\mathbf{B},\{\mathbf{b}_a\})|A_i\rangle$ in a space span by impact parameters $\{\mathbf{b}_a\}$. Clearly, in the black-disk limit, corresponding to the asymptotically high energies $s\to\infty$, this deviation vanishes because $\Gamma^{pN}(s,\mathbf{B},\{\mathbf{b}_a\}) \to 1$ for $|\mathbf{B}-\mathbf{b}_a| < R_A$ and is zero otherwise; see Eq. (5). The standard deviation is a measure of quantum fluctuations near the mean-field value.

Because $\Gamma^{pN}(s,\{\mathbf{b}_a\})$ is approximately real, we have using (5)

$$\begin{aligned}(\Gamma^{pA}(s,\mathbf{B},\{\mathbf{b}_a\})^2 &= \left(1 - \prod_{a=1}^{A}[1-\Gamma^{pN}(s,\mathbf{B}-\mathbf{b}_a)]\right)^2 \\ &= 1 - 2\prod_{a=1}^{A}[1-\Gamma^{pN}(s,\mathbf{B}-\mathbf{b}_a)] \\ &\quad + \prod_{a=1}^{A}[1-\Gamma^{pN}(s,\mathbf{B}-\mathbf{b}_a)]^2\end{aligned} \tag{18}$$

Averaging over the nucleus and taking the large A limit we obtain

$$\begin{aligned}&\langle A_i||\Gamma^{pA}(s,\mathbf{B},\{\mathbf{b}_a\})|^2|A_i\rangle \\ &\quad= 1 - 2\,e^{-\int d^2b\Gamma^{pN}(s,\mathbf{B}-\mathbf{b})\rho T_A(b)} \\ &\qquad + e^{-\int d^2b[2\Gamma^{pN}(s,\mathbf{B}-\mathbf{b})-(\Gamma^{pN}(s,\mathbf{B}-\mathbf{b}))^2]\rho T_A(b)} \\ &\quad= 1 - 2e^{-\frac{1}{2}\sigma_{\mathrm{tot}}^{pN}(s)\,\rho T_A(\mathbf{b})} + e^{-\sigma_{\mathrm{in}}^{pN}(s)\,\rho T_A(\mathbf{b})},\end{aligned} \tag{19}$$

where we used Eq. (12) and denoted the inelastic pN cross section as $\sigma_{\mathrm{in}}^{pN}(s)$. Substituting Eq. (19) into Eq. (17) and using Eq. (16) we derive

$$\sigma_{\mathrm{ID}}^{pA}(s) = \int d^2b e^{-\sigma_{\mathrm{in}}^{pN}(s)\,\rho T_A(\mathbf{b})}\left[1 - e^{-\sigma_{\mathrm{el}}^{pN}(s)\,\rho T_A(\mathbf{b})}\right]. \tag{20}$$

Elastic cross section $\sigma_{\mathrm{el}}^{pN}$, which appears in Eq. (20), can be found by taking square of (12) and integrating over the impact parameter:

$$\begin{aligned}\sigma_{\mathrm{el}}^{pN} &= \int d^2b |\Gamma^{pN}(s,\mathbf{b})|^2 \\ &= \frac{1}{4}\left(\sigma_{\mathrm{tot}}^{pN}\right)^2 \int d^2b S_p^2(\mathbf{b}) = \frac{\left(\sigma_{\mathrm{tot}}^{pN}\right)^2}{8\pi R_p^2},\end{aligned} \tag{21}$$

where we used (13).

It is seen from Eqs. (16) and (20) that because the pN cross sections increase with energy, at asymptotically high energies the incoherent diffraction cross section vanishes, whereas the coherent one reaches a half of the total cross section. This well-known conclusion is a consequence of unitarity of the scattering amplitude and thus is independent of interaction details.

III. DIFFRACTION IN THE DIPOLE MODEL

It is phenomenologically reasonable to approximate the proton light-cone wave-function (away from fragmentation regions) by a system of color dipoles [3,34,35]. If separation of quark and antiquark is small, one can apply the perturbation theory to calculate the scattering amplitude of quarkonium on the nucleus. It was demonstrated by Mueller in Ref. [21] that at high energies the $q\bar{q}A$ forward elastic-scattering amplitude

takes exactly the same form as Eq. (15) with the pA cross section replaced by the $q\bar{q}A$ one. By virtue of the optical theorem, the total quarkonium–nucleus cross section reads

$$\sigma_{\rm tot}^{q\bar{q}A}(s;\mathbf{r}) = 2\int d^2b N_A(\mathbf{r},\mathbf{b},Y) = 2\int d^2b\left[1-e^{-\frac{1}{2}\sigma_{\rm tot}^{q\bar{q}N}(s;\mathbf{r})\rho T_A(\mathbf{b})}\right], \quad (22)$$

where

$$N_A(\mathbf{r},\mathbf{b},Y) = {\rm Re}\Gamma_{ii}^{q\bar{q}A}(s,\mathbf{b};\mathbf{r}) \quad (23)$$

is the imaginary part of the forward elastic $q\bar{q}A$-scattering amplitude and $Y = \ln(1/x) = \ln(s/s_0)$ is rapidity with s_0 a reference energy scale. Equation (22) is called the Glauber–Mueller formula. Let us note that it is far from obvious that the high-energy amplitude in Eq. (22) must have the same form as the low-energy one (15). In this correspondence it is crucial that the color dipoles are identified as the relevant degrees if freedom at high energies. Equation (22) holds when $\ln(m_N R_A) \ll Y \ll 1/\alpha_s$, where m_N is a nucleon mass. This condition guarantees that the coherence length l_c is much larger than the nuclear radius [see Eq. (30)] and that the low-x gluon evolution is suppressed. In this case $q\bar{q}N$ cross section can be calculated in the Born approximation (two-gluon exchange) as

$$\sigma_{\rm tot}^{q\bar{q}N}(s;\mathbf{r}) = \frac{\alpha_s}{N_c}\pi^2\mathbf{r}^2 xG(x,1/\mathbf{r}^2), \quad (24)$$

with the gluon distribution function

$$xG(x,1/\mathbf{r}^2) = \frac{\alpha_s C_F}{\pi}\ln\frac{1}{\mathbf{r}^2\mu^2}, \quad (25)$$

where μ is an infrared cutoff. We can rewrite (24) in terms of the *gluon* saturation scale Q_{s0}^2 defined as

$$Q_{s0}^2 = \frac{4\pi^2\alpha_s N_c}{N_c^2-1}\rho T_A(\mathbf{b})\, xG(x,1/\mathbf{r}^2). \quad (26)$$

Subscript 0 indicates that the low-x evolution is suppressed. Equation (25) implies that in the Born approximation the $q\bar{q}N$ total cross section (24) and hence the saturation scale (26) are energy independent. Using this definition we have

$$\rho T_A(\mathbf{b})\,\sigma_{\rm tot}^{q\bar{q}N}(s;\mathbf{r}) = \frac{C_F}{2N_c}\mathbf{r}^2 Q_{s0}^2, \quad (27)$$

where $C_F = (N_c^2-1)/(2N_c)$. Substituting Eq. (27) into Eq. (22) we derive another representation of the total quarkonium–nucleus cross section

$$\sigma_{\rm tot}^{q\bar{q}A}(s;\mathbf{r}) = 2\int d^2b\left(1-e^{-\frac{1}{4}\frac{C_F}{N_c}\mathbf{r}^2 Q_{s0}^2}\right). \quad (28)$$

The integrand of Eq. (28) represents the propagator of quarkonium $q\bar{q}$ of size $\mathbf{b}$ through the nucleus at impact parameter $\mathbf{b}$. Because $\sigma_{\rm tot}^{q\bar{q}N} \sim \alpha_s^2$ and $\rho T_A(\mathbf{b}) \sim A^{1/3}$ Eq. (28) sums up powers of $\alpha_s^2 A^{1/3}$. It has been shown by Kovchegov that this corresponds to the coherent scattering of $q\bar{q}$ off the quasiclassical field of the nucleus [7]. This is possible only if the coherence length l_c of the $q\bar{q}$ pair is much larger than the nuclear radius. This condition certainly holds at RHIC energies. In the quasiclassical approximation the coherent diffraction cross section is given by [cf. Eq. (16)]

$$\sigma_{\rm CD}^{q\bar{q}A}(s;\mathbf{r}) = \int d^2b\left|\Gamma_{ii}^{q\bar{q}A}(s,\mathbf{b};\mathbf{r})\right|^2 = \int d^2b\left(1-e^{-\frac{1}{4}\frac{C_F}{N_c}Q_{s0}^2\mathbf{r}^2}\right)^2, \quad (29)$$

Equation (29) represents the leading contribution to the diffraction cross section in the quasiclassical field strength. On the contrary, the incoherent diffraction cross section, see Eq. (20), vanishes in this mean-field approximation because $\sigma_{\rm el}^{q\bar{q}N}\rho T_A(\mathbf{b}) \sim \alpha_s{}^4 A^{1/3} \sim \alpha_s^2 \ll 1$. Vanishing of the incoherent diffraction cross section can also be seen directly from Eq. (17). It is a consequence of vanishing relative fluctuations at large occupation numbers of classical fields. This effect has recently been studied within the Glauber framework (see Sec. II) in [35–37].

Let us emphasize, to avoid possible confusion, that the semantic distinction between the coherent and incoherent diffraction concerns the nucleus target staying intact or breaking down in the collision. As far as the coherence length is concerned, at high enough energies such that $l_c \gg R_A$ the *scattering* is coherent for both coherent and incoherent diffraction. However, unlike the incoherent diffraction that can happen in the incoherent scattering at low energies (provided only that $l_c \gg R_N$), the coherent diffraction is possible only if the scattering is coherent over the entire nucleus.

IV. DIFFRACTIVE GLUON PRODUCTION

A. Coherent diffractive gluon production

Consider coherent diffractive production of a gluon of momentum k in $q\bar{q}A$ collision. As mentioned, coherent diffraction is possible only if the coherence length l_c of the emitted gluon with momentum k is larger than the nucleus size R_A (in the nucleus rest frame):

$$l_c = \frac{k_+}{\mathbf{k}^2} \gg R_A, \quad (30)$$

where $+$ indicates the light-cone direction of the incoming proton. The invariant mass of the produced system is given by $M^2 = \mathbf{k}^2/x$, where $x = k_+/p_+$ and p is the proton momentum. Substituting these equations in Eq. (30) yields the following condition on the mass of the diffractive system:

$$M^2 \ll \frac{p_+}{R_A} = \frac{s}{R_A m_p}, \quad (31)$$

where $\sqrt{s}$ is the center-of-mass energy of the proton-nucleon collision and m_p is proton mass.

Coherent diffractive gluon production off the large nucleus was calculated in Refs. [25,38,39]. The corresponding cross section reads

$$\frac{d\sigma_{\rm CD}(k,y)}{d^2k dy} = \frac{1}{(2\pi)^2}\int d^2b d^2z_1 d^2z_2\,\Phi^{q\bar{q}}(\mathbf{x},\mathbf{y},\mathbf{z}_1,\mathbf{z}_2)e^{-i\mathbf{k}\cdot(\mathbf{z}_1-\mathbf{z}_2)} \times\left[\Gamma_{ii}^{q\bar{q}GA}(s,\mathbf{b};\mathbf{x},\mathbf{y},\mathbf{z}_1)-\Gamma_{ii}^{q\bar{q}A}(s,\mathbf{b};\mathbf{x},\mathbf{y})\right] \times\left[\Gamma_{ii}^{q\bar{q}GA}(s,\mathbf{b};\mathbf{x},\mathbf{y},\mathbf{z}_2)-\Gamma_{ii}^{q\bar{q}A}(s,\mathbf{b};\mathbf{x},\mathbf{y})\right], \quad (32)$$

where the $q\bar{q} \to q\bar{q}G$ light-cone wave function $\Phi^{q\bar{q}}$ is given by

$$\Phi^{q\bar{q}}(\mathbf{x},\mathbf{y},\mathbf{z}_1,\mathbf{z}_2) = \frac{\alpha_s C_F}{\pi^2}\left(\frac{\mathbf{z}_1-\mathbf{x}}{|\mathbf{z}_1-\mathbf{x}|^2} - \frac{\mathbf{z}_1-\mathbf{y}}{|\mathbf{z}_1-\mathbf{y}|^2}\right) \times \left(\frac{\mathbf{z}_2-\mathbf{x}}{|\mathbf{z}_2-\mathbf{x}|^2} - \frac{\mathbf{z}_2-\mathbf{y}}{|\mathbf{z}_2-\mathbf{y}|^2}\right). \quad (33)$$

The $q\bar{q}$ scattering amplitude $\Gamma^{q\bar{q}A}_{ii,\sigma}(s,\mathbf{b})$ is given by Eq. (29), while the $q\bar{q}G$ one was calculated in Refs. [39–41] and reads

$$\begin{aligned}\Gamma^{q\bar{q}GA}_{ii,\sigma}(s,\mathbf{b};\mathbf{x},\mathbf{y},\mathbf{z}_\sigma) &= \langle A_i|\Gamma^{q\bar{q}GA}_{\sigma}(s,\mathbf{B},\{\mathbf{b}_a\};\mathbf{x},\mathbf{y},\mathbf{z}_\sigma)|A_i\rangle \\ &= 1 - e^{-\frac{1}{2}\sigma^{q\bar{q}GN}_{\rm tot}(s;\mathbf{x},\mathbf{y},\mathbf{z}_\sigma)\,\rho T_A(\mathbf{b})} \\ &= 1 - e^{-\frac{1}{8}(\mathbf{x}-\mathbf{z}_\sigma)^2 Q^2_{s0} - \frac{1}{8}(\mathbf{y}-\mathbf{z}_\sigma)^2 Q^2_{s0} - \frac{1}{8N_c^2}(\mathbf{x}-\mathbf{y})^2 Q^2_{s0}}, \end{aligned} \quad (34)$$

where $\mathbf{x}$, $\mathbf{y}$, and $\mathbf{z}_\sigma$ are the transverse coordinates of quark, antiquark, and gluon, respectively; $\sigma = 1$ in the amplitude and $\sigma = 2$ in the complex conjugated one. For future reference, note that we can express the $q\bar{q}GN$ total cross section in terms of the $q\bar{q}N$ one given by (27)

$$\sigma^{q\bar{q}GN}_{\rm tot}(s;\mathbf{x},\mathbf{y},\mathbf{z}_\sigma) = \frac{N_c}{2C_F}\left[\sigma^{q\bar{q}N}_{\rm tot}(s;\mathbf{x}-\mathbf{z}_\sigma) + \sigma^{q\bar{q}N}_{\rm tot}(s;\mathbf{y}-\mathbf{z}_\sigma) - \frac{1}{N_c^2}\sigma^{q\bar{q}N}_{\rm tot}(s;\mathbf{x}-\mathbf{y})\right], \quad (35)$$

where we explicitly indicated the dipole size and energy dependence of the $q\bar{q}N$ total cross section.

Depending on the relation between the gluon emission time τ_σ and the interaction time τ'_σ in the amplitude and in the complex conjugated (c.c.) amplitude there are four possible products of the $q\bar{q}$ and $q\bar{q}G$ amplitudes appearing in the second line of Eq. (32). Explicitly,

$$\begin{aligned}&\langle A_i|\Gamma^{q\bar{q}A}(s,\mathbf{B},\{\mathbf{b}_a\};\mathbf{x},\mathbf{y})|A_i\rangle^\dagger \\ &\quad\times\langle A_i|\Gamma^{q\bar{q}A}(s,\mathbf{B},\{\mathbf{b}_a\};\mathbf{x},\mathbf{y})|A_i\rangle \\ &\quad+\langle A_i|\Gamma^{q\bar{q}GA}(s,\mathbf{B},\{\mathbf{b}_a\};\mathbf{x},\mathbf{y},\mathbf{z}_1)|A_i\rangle^\dagger \\ &\quad\times\langle A_i|\Gamma^{q\bar{q}GA}(s,\mathbf{B},\{\mathbf{b}_a\};\mathbf{x},\mathbf{y},\mathbf{z}_2)|A_i\rangle \\ &\quad-\langle A_i|\Gamma^{q\bar{q}A}(s,\mathbf{B},\{\mathbf{b}_a\};\mathbf{x},\mathbf{y})|A_i\rangle^\dagger \\ &\quad\times\langle A_i|\Gamma^{q\bar{q}GA}(s,\mathbf{B},\{\mathbf{b}_a\};\mathbf{x},\mathbf{y},\mathbf{z}_2)|A_i\rangle \\ &\quad-\langle A_i|\Gamma^{q\bar{q}GA}(s,\mathbf{B},\{\mathbf{b}_a\};\mathbf{x},\mathbf{y},\mathbf{z}_1)|A_i\rangle^\dagger \\ &\quad\times\langle A_i|\Gamma^{q\bar{q}A}(s,\mathbf{B},\{\mathbf{b}_a\};\mathbf{x},\mathbf{y})|A_i\rangle. \end{aligned} \quad (36)$$

B. Incoherent diffractive gluon production

To calculate the propagators in the case of incoherent diffraction we need to consider each one of the four cases shown in Eq. (36) and follow the by now familiar steps of Eqs. (17)–(20). Consider, for example, gluon emission before the interaction in the amplitude and in the c.c. one, i.e., $\tau_\sigma < \tau'_\sigma$ for $\sigma = 1, 2$. The detailed calculation is presented in the Appendix. The result is [cf. Eq. (20)]

$$\begin{aligned}&\sum_{f\neq i}\langle A_f|\Gamma^{q\bar{q}GA}(s,\mathbf{B},\{\mathbf{b}_a\};\mathbf{x},\mathbf{y},\mathbf{z}_1)|A_i\rangle^\dagger\langle A_f|\Gamma^{q\bar{q}GA}_2(s,\mathbf{B},\{\mathbf{b}_a\};\mathbf{x},\mathbf{y},\mathbf{z}_2)|A_i\rangle \\ &\quad= e^{-\frac{1}{2}[\sigma^{q\bar{q}GN}_{\rm tot}(s;\mathbf{x},\mathbf{y},\mathbf{z}_1)+\sigma^{q\bar{q}GN}_{\rm tot}(s;\mathbf{x},\mathbf{y},\mathbf{z}_2)-\frac{1}{4\pi R_p^2}\sigma^{q\bar{q}GN}_{\rm tot}(s;\mathbf{x},\mathbf{y},\mathbf{z}_1)\,\sigma^{q\bar{q}GN}_{\rm tot}(s;\mathbf{x},\mathbf{y},\mathbf{z}_2)]\,\rho T_A(\mathbf{b})} \\ &\qquad\times\left\{1 - e^{-\frac{1}{2}\frac{1}{4\pi R_p^2}\sigma^{q\bar{q}GN}_{\rm tot}(s;\mathbf{x},\mathbf{y},\mathbf{z}_1)\,\sigma^{q\bar{q}GN}_{\rm tot}(s;\mathbf{x},\mathbf{y},\mathbf{z}_2)\,\rho T_A(\mathbf{b})}\right\}. \end{aligned} \quad (37)$$

This result holds in the quasiclassical approximation $\alpha_s^2 A^{1/3} \sim 1$. Therefore, contribution of elastic processes to Eq. (37) are of the order

$$\left(\sigma^{q\bar{q}GN}_{\rm tot}\right)^2 \rho T_A(\mathbf{b}) \sim {\alpha_s}^4 A^{1/3} \sim \alpha_s^2.$$

It is suppressed compared to the contribution of inelastic processes that are of order $\alpha_s^2 A^{1/3} \sim 1$. Note that the contribution to the incoherent diffraction cross section given by Eq. (37) vanishes with vanishing elastic $q\bar{q}N$ cross section. Thus, we expand the expression in the curly brackets of Eq. (37), keeping the leading elastic term. We derive

$$\begin{aligned}&\sum_{f\neq i}\langle A_f|\Gamma^{q\bar{q}GA}(s,\mathbf{B},\{\mathbf{b}_a\};\mathbf{x},\mathbf{y},\mathbf{z}_1)|A_i\rangle^\dagger \\ &\quad\times\langle A_f|\Gamma^{q\bar{q}GA}(s,\mathbf{B},\{\mathbf{b}_a\};\mathbf{x},\mathbf{y},\mathbf{z}_2)|A_i\rangle \\ &\approx \frac{\rho T_A(\mathbf{b})}{8\pi R_p^2}\,\sigma^{q\bar{q}GN}_{\rm tot}(s;\mathbf{x},\mathbf{y},\mathbf{z}_1)\,\sigma^{q\bar{q}GN}_{\rm tot}(s;\mathbf{x},\mathbf{y},\mathbf{z}_2) \\ &\quad\times e^{-\frac{1}{2}[\sigma^{q\bar{q}GN}_{\rm tot}(s;\mathbf{x},\mathbf{y},\mathbf{z}_1)+\sigma^{q\bar{q}GN}_{\rm tot}(s;\mathbf{x},\mathbf{y},\mathbf{z}_2)]\,\rho T_A(\mathbf{b})}. \end{aligned} \quad (38)$$

This approximation is valid at not too high energies satisfying

$$\frac{1}{8\pi R_p^2}\left(\sigma^{q\bar{q}GN}_{\rm tot}\right)^2 \rho T_A(\mathbf{b}) \ll 1. \quad (39)$$

Let us for simplicity consider a cylindrical nucleus for which $\rho T_A(\mathbf{b}) = 2A/(\pi R_A^2)$. Because $R_A = A^{1/3} R_p$ and taking into account that $\frac{1}{2}\sigma^{q\bar{q}GN}_{\rm tot}\rho T_A(\mathbf{b}) = \frac{1}{4}\,Q_s^2 r^2$ for $N_c \gg 1$ [see Eqs. (22) and (29)] we can rewrite (39) as

$$\tfrac{1}{4}Q_s^2 r^2 \ll 2A^{1/6}. \quad (40)$$

The saturation effects in the nucleus become important when $\frac{1}{4}Q_s^2 r^2 \gtrsim 1$. At rapidities $Y \sim 1/\alpha_s$ the low x evolution effects give rise to the energy dependence of the saturation scale. Let Y_1 be the rapidity at which $\frac{1}{4}Q_s^2 r^2 = 1$ and Y_2 be the rapidity at which $\frac{1}{4}Q_s^2 r^2 = 2A^{1/6}$. Because $Q_s^2 \propto e^{\lambda Y}$ [42] we obtain $Y_2 - Y_1 = \lambda^{-1}\ln(2A^{1/6})$. Using the phenomenological value $\lambda = 0.25$ for the Gold nucleus $A = 197$ we find that there are

$Y_2 - Y_1 \approx 6$ units of rapidity between Y_1 where the saturation effects become important and Y_2 where the expansion (38) breaks down. This provides quite wide kinematic window in which approximation (39) holds.

Other three cases corresponding to different relations between τ_σ and τ'_σ can be worked out in a similar way. The result for the cross section of incoherent diffractive gluon production takes form

$$\frac{d\sigma_{\rm ID}(k,\,y)}{d^2k\,dy} = \frac{1}{(2\pi)^2}\,\frac{1}{8\pi R_p^2}\int d^2b\,d^2z_1\,d^2z_2\,\Phi^{q\bar q}(\mathbf{x},\,\mathbf{y},\,\mathbf{z}_1,\,\mathbf{z}_2) \times e^{-i\mathbf{k}\cdot(\mathbf{z}_1-\mathbf{z}_2)}\,\rho T_A(\mathbf{b}) \times \Big[\sigma_{\rm tot}^{q\bar qGN}(s;\mathbf{x},\,\mathbf{y},\,\mathbf{z}_1)e^{-\frac{1}{2}\sigma_{\rm tot}^{q\bar qGN}(s;\mathbf{x},\mathbf{y},\mathbf{z}_1)\,\rho T_A(\mathbf{b})} - \sigma_{\rm tot}^{q\bar qN}(s;\mathbf{x},\,\mathbf{y})e^{-\frac{1}{2}\sigma_{\rm tot}^{q\bar qN}(s;\mathbf{x},\mathbf{y})\,\rho T_A(\mathbf{b})}\Big] \times \Big[\sigma_{\rm tot}^{q\bar qGN}(s;\mathbf{x},\,\mathbf{y},\,\mathbf{z}_2)e^{-\frac{1}{2}\sigma_{\rm tot}^{q\bar qGN}(s;\mathbf{x},\mathbf{y},\mathbf{z}_2)\,\rho T_A(\mathbf{b})} - \sigma_{\rm tot}^{q\bar qN}(s;\mathbf{x},\,\mathbf{y})e^{-\frac{1}{2}\sigma_{\rm tot}^{q\bar qN}(s;\mathbf{x},\mathbf{y})\,\rho T_A(\mathbf{b})}\Big]. \tag{41}$$

V. LOW-x EVOLUTION

A. Incoherent diffraction

The results derived in the previous section can be generalized beyond the quasiclassical level to include the low-x evolution. This procedure follows the general strategy developed in Ref. [43] and has been used in Refs. [1,2] to derive the expression for the coherent diffractive gluon production in onium-nucleus collisions. In this we section we derive an analogous expressions for the incoherent diffractive gluon production. For applying this general strategy it is important that formula Eq. (38) can be factorized in a product of two expressions, one depending on the gluon coordinate $\mathbf{z}_1$ and another one on $\mathbf{z}_2$.

The low-x gluon evolution in the nucleus at large N_c is taken into account by the following two substitutions in Eq. (41): (i) the exponents are replaced by the forward elastic $q\bar qA$ scattering amplitude $N_A(\mathbf{r},\mathbf{b},Y)$ [43]

$$e^{-\frac{1}{2}\sigma_{\rm tot}^{q\bar qN}(s;\mathbf{r})\,\rho T_A(\mathbf{b})} \to 1 - N_A(\mathbf{r},\mathbf{b},Y). \tag{42}$$

$N_A(\mathbf{r},\mathbf{b},Y)$ evolves toward higher rapidities Y, i.e., lower x, according to the nonlinear BK evolution equation [8,14] from its initial condition, given by Eq. (22) at some rapidity $Y = Y_0$; (ii) the factors linear in $\sigma_{\rm tot}^{q\bar qN}$ have emerged in expansion (38) where the terms of higher order (i.e., multiple scattering) in the elastic amplitude were neglected. Therefore, they are replaced by the forward elastic $q\bar qN$-scattering amplitude $N_p(\mathbf{r},\mathbf{b},Y)$ that evolves according to the linear BFKL equation [44,45]. It is defined similarly to Eq. (23) [see Eq. (12)]

$$N_p(\mathbf{r},\mathbf{b},Y) = {\rm Re}\Gamma^{q\bar qp}(s,\mathbf{b};\mathbf{r}) = \tfrac{1}{2}\sigma_{\rm tot}^{q\bar qp}(s;\mathbf{r})\,S_p(\mathbf{b}). \tag{43}$$

Recall that in the heavy nucleus environment the impact parameter dependence of $q\bar q\,p$ cross section can be neglected; see Eq. (14). Thus, using Eq. (13) we have

$$\sigma_{\rm tot}^{q\bar qN}(s;\mathbf{r}) \to 2\pi R_p^2 N_p(\mathbf{r},0,Y) \tag{44}$$

in agreement with the optical theorem. The factors linear in the $q\bar qGN$ cross section are replaced similarly using (35). Substituting Eqs. (42) and (44) into Eq. (41) using Eq. (35) (in the multicolor $N_c \gg 1$ limit) yields

$$\begin{aligned}\frac{d\sigma_{\rm ID}(k,\,y)}{d^2k\,dy} = \frac{1}{(2\pi)^2}\,\frac{\pi R_p^2}{2}\int d^2b\,d^2z_1\,d^2z_2\,\Phi^{q\bar q}(\mathbf{x},\,\mathbf{y},\,\mathbf{z}_1,\,\mathbf{z}_2)\\ \times \rho T_A(\mathbf{b})e^{-i\mathbf{k}\cdot(\mathbf{z}_1-\mathbf{z}_2)}\\ \times \{[1 - N_A(\mathbf{z}_1-\mathbf{x},\mathbf{b},y)]\\ \times [1 - N_A(\mathbf{z}_1-\mathbf{y},\mathbf{b},y)][N_p(\mathbf{z}_1-\mathbf{x},0,y)\\ + N_p(\mathbf{z}_1-\mathbf{y},0,y)]\\ - [1 - N_A(\mathbf{x}-\mathbf{y},\mathbf{b},y)]N_p(\mathbf{x}-\mathbf{y},0,y)\}\\ \times \{[1 - N_A(\mathbf{z}_2-\mathbf{x},\mathbf{b},y)]\\ \times [1 - N_A(\mathbf{z}_2-\mathbf{y},\mathbf{b},y)][N_p(\mathbf{z}_2-\mathbf{x},0,y)\\ + N_p(\mathbf{z}_2-\mathbf{y},0,y)]\\ - [1 - N_A(\mathbf{x}-\mathbf{y},\mathbf{b},y)]N_p(\mathbf{x}-\mathbf{y},0,y)\}.\end{aligned} \tag{45}$$

We can write (45) in a more compact form introducing the following two-dimensional vector

$$\begin{aligned}&\mathbf{I}_{\rm ID}(\mathbf{x}-\mathbf{y},\,\mathbf{b},\,y;\mathbf{k})\\ &= \int d^2z\left(\frac{\mathbf{z}-\mathbf{x}}{|\mathbf{z}-\mathbf{x}|^2} - \frac{\mathbf{z}-\mathbf{y}}{|\mathbf{z}-\mathbf{y}|^2}\right)e^{-i\mathbf{k}\cdot\mathbf{z}}\\ &\quad\times\{[1 - N_A(\mathbf{z}-\mathbf{x},\mathbf{b},y)][1 - N_A(\mathbf{z}-\mathbf{y},\mathbf{b},y)]\\ &\quad\times[N_p(\mathbf{z}-\mathbf{x},0,y) + N_p(\mathbf{z}-\mathbf{y},0,y)]\\ &\quad- [1 - N_A(\mathbf{x}-\mathbf{y},\mathbf{b},y)]N_p(\mathbf{x}-\mathbf{y},0,y)\}.\end{aligned} \tag{46}$$

Then,

$$\frac{d\sigma_{\rm ID}(k,\,y)}{d^2k\,dy} = \frac{\alpha_s C_F}{\pi^2}\,\frac{1}{(2\pi)^2}\,\frac{\pi R_p^2}{2} \times \int d^2b\;\rho T_A(\mathbf{b})|\mathbf{I}_{\rm ID}(\mathbf{x}-\mathbf{y},\mathbf{b},y;\mathbf{k})|^2. \tag{47}$$

So far we have discussed the gluon evolution in the rapidity interval y between the emitted gluon and the target nucleus. The low-x evolution also occurs in the rapidity interval $Y - y$ between the incident quarkonium $q\bar q$ and the emitted gluon (we now denote by Y the rapidity between the quarkonium and the nucleus and by y the inclusive gluon rapidity). The low-x evolution in the incident quarkonium is taken into account by convoluting (47) with the dipole density $n_1(\mathbf{r},\mathbf{r}',\mathbf{B}-\mathbf{b},Y-y)$, where $\mathbf{r} = \mathbf{x} - \mathbf{y}$:

$$\frac{d\sigma_{\rm ID}(k,\,y)}{d^2k\,dy} = \frac{\alpha_s C_F}{\pi^2}\,\frac{\pi R_p^2}{2(2\pi)^2}\int d^2b\int d^2B \times \int d^2r' n_1(\mathbf{r},\mathbf{r}',\mathbf{B}-\mathbf{b},Y-y)\rho T_A(\mathbf{b}) \times |\mathbf{I}_{\rm ID}(\mathbf{r},\mathbf{b},y;\mathbf{k})|^2. \tag{48}$$

The dipole density $n_1(\mathbf{r}, \mathbf{r}, \mathbf{B}-\mathbf{b}, Y-y)$ has the meaning of the number of dipoles of size $\mathbf{r}'$ at rapidity $Y-y$ and impact parameter $\mathbf{b}$ generated by evolution from the original dipole $\mathbf{r}$ having rapidity Y and impact parameter $\mathbf{B}$ [21]. It obeys the BFKL equation [44,45]. As the interval $Y-y$ increases the quarkonium wave function involves increasing number of dipoles. Although the dipole size distribution diffuses according to the BFKL equation, the typical dipole size is much smaller than the nuclear radius R_A, i.e., $|\mathbf{B}-\mathbf{b}| \ll b$. Integrating over $\mathbf{B}-\mathbf{b}$ in this approximation we derive

$$\frac{d\sigma_{\rm ID}(k,y)}{d^2k\,dy} = \frac{\alpha_s C_F}{\pi^2}\frac{\pi R_p^2}{2(2\pi)^2}\int d^2b \int d^2r' n_p(\mathbf{r},\mathbf{r}',Y-y) \times \rho T_A(\mathbf{b})|\mathbf{I}_{\rm ID}(\mathbf{r},\mathbf{b},y;\mathbf{k})|^2, \quad (49)$$

where we defined [1,2]

$$n_p(\mathbf{r},\mathbf{r}',Y) = \int n_1(\mathbf{r},\mathbf{r}',\mathbf{b}',Y)d^2b'. \quad (50)$$

Equations (49) and (46) constitute the main result of this article.

B. Coherent diffraction

The cross section for the coherent diffractive gluon production including the low-x evolution was derived in Refs. [1,2]. It can be written similarly to Eq. (49) [1,2]:

$$\frac{d\sigma_{\rm CD}(k,y)}{d^2k\,dy} = \frac{\alpha_s C_F}{\pi^2}\frac{1}{(2\pi)^2}\int d^2b \int d^2r' n_p(\mathbf{r},\mathbf{r}',Y-y) \times |\mathbf{I}_{\rm CD}(\mathbf{r},\mathbf{b},y;\mathbf{k})|^2, \quad (51)$$

where

$$\mathbf{I}_{\rm CD}(\mathbf{x}-\mathbf{y},\mathbf{b},y;\mathbf{k}) = \int d^2z \left(\frac{\mathbf{z}-\mathbf{x}}{|\mathbf{z}-\mathbf{x}|^2}-\frac{\mathbf{z}-\mathbf{y}}{|\mathbf{z}-\mathbf{y}|^2}\right) e^{-i\mathbf{k}\cdot\mathbf{z}} \times [-N_A(\mathbf{z}-\mathbf{x},\mathbf{b},y) - N_A(\mathbf{z}-\mathbf{y},\mathbf{b},y) + N_A(\mathbf{x}-\mathbf{y},\mathbf{b},y) + N_A(\mathbf{z}-\mathbf{x},\mathbf{b},y)\,N_A(\mathbf{z}-\mathbf{y},\mathbf{b},y)]. \quad (52)$$

In Refs. [1,2] we presented a detailed analytical and numerical analysis of the the coherent diffractive gluon production.

C. Logarithmic approximation

To obtain a working model for numerical calculations, it is useful to estimate $\mathbf{I}_{\rm ID}(\mathbf{r},\mathbf{b},y;\mathbf{k})$ in the logarithmic approximation. First, let us change the integration variable $\mathbf{w}=\mathbf{z}-\mathbf{y}$ and define an auxiliary function [1,2]

$$Q_{\rm ID}(\mathbf{r}',y;\mathbf{k}) = \int \frac{d^2w}{w^2}e^{i\mathbf{k}\cdot\mathbf{w}}\{[1-N_A(\mathbf{r}',\mathbf{b},y)]N_p(\mathbf{r}',0,y) - [1-N_A(\mathbf{w}-\mathbf{r}',\mathbf{b},y)][1-N_A(\mathbf{w},\mathbf{b},y)] \times [N_p(\mathbf{w}-\mathbf{r}',0,y)+N_p(\mathbf{w},0,y)]\}. \quad (53)$$

With this definition (46) becomes

$$\mathbf{I}_{\rm ID}(\mathbf{r},\mathbf{b},y;\mathbf{k}) = -e^{-i\mathbf{k}\cdot\mathbf{r}}\,i\nabla_{\mathbf{k}}Q_{\rm ID}(\mathbf{r}',y;\mathbf{k}) + e^{i\mathbf{k}\cdot\mathbf{r}}\,i\nabla_{\mathbf{k}}Q^*_{\rm ID}(\mathbf{r}',y;\mathbf{k}). \quad (54)$$

In the logarithmic approximation $Q_{\rm ID}(\mathbf{r}',y;\mathbf{k})$ is a real function [1,2]. Therefore, we can write

$$|\mathbf{I}_{\rm ID}(\mathbf{r},\mathbf{b},y;\mathbf{k})|^2 = 4\sin^2\left(\tfrac{1}{2}\,\mathbf{k}\cdot\mathbf{r}'\right)[\nabla_{\mathbf{k}}Q_{\rm ID}(\mathbf{r}',y;\mathbf{k})]^2. \quad (55)$$

Notice that the integral over $\mathbf{z}$ in Eq. (46) is dominated by the region $w<1/k$ because otherwise the integrand is a rapidly oscillation function. Restricting integration to this region yields results valid as long as the scales $1/r'$, Q_s and k are strongly ordered [1,2]. Operating with $\nabla_{\mathbf{k}}$ on $Q_{\rm ID}(\mathbf{r}',y;\mathbf{k})$ yields

$$\begin{aligned}\nabla_{\mathbf{k}}Q_{\rm ID}(\mathbf{r}',y;\mathbf{k}) &= -\frac{\mathbf{k}}{k^3}\frac{\partial}{\partial k^{-1}}Q_{\rm ID}(\mathbf{r}',y;\mathbf{k})\\ &= -2\pi\frac{\mathbf{k}}{k^2}\{[1-N_A(\mathbf{r}',\mathbf{b},y)]N_p(\mathbf{r}',0,y)\\ &\quad -[1-N_A(\mathbf{k}\,k^{-2}-\mathbf{r}',\mathbf{b},y)]\\ &\quad \times[1-N_A(\mathbf{k}\,k^{-2},\mathbf{b},y)]\\ &\quad \times[N_p(\mathbf{k}\,k^{-2}-\mathbf{r}',0,y)\\ &\quad +N_p(\mathbf{k}\,k^{-2},0,y)]\}. \end{aligned} \quad (56)$$

Analogously, in the coherent diffraction case we define

$$Q_{\rm CD}(\mathbf{r}',y;\mathbf{k}) = \int\frac{d^2w}{w^2}e^{i\mathbf{k}\cdot\mathbf{w}}\{N_A(\mathbf{w}-\mathbf{r}',\mathbf{b},y) + N_A(\mathbf{w},\mathbf{b},y) - N_A(\mathbf{r}',\mathbf{b},y) - N_A(\mathbf{w}-\mathbf{r}',\mathbf{b},y)\,N_A(\mathbf{w},\mathbf{b},y)\}. \quad (57)$$

Then, in the logarithmic approximation,

$$\nabla_{\mathbf{k}}Q_{\rm CD}(\mathbf{r}',y;\mathbf{k}) = -2\pi\frac{\mathbf{k}}{k^2}\{-N_A(\mathbf{r}',\mathbf{b},y) + N_A(\mathbf{k}\,k^{-2}-\mathbf{r}',\mathbf{b},y)+N_A(\mathbf{k}\,k^{-2},\mathbf{b},y) - N_A(\mathbf{k}\,k^{-2}-\mathbf{r}',\mathbf{b},y)\,N_A(\mathbf{k}\,k^{-2},\mathbf{b},y)\}. \quad (58)$$

Similarly (55) becomes

$$|\mathbf{I}_{\rm CD}(\mathbf{r},\mathbf{b},y;\mathbf{k})|^2 = 4\sin^2\left(\tfrac{1}{2}\,\mathbf{k}\cdot\mathbf{r}'\right)[\nabla_{\mathbf{k}}Q_{\rm CD}(\mathbf{r}',y;\mathbf{k})]^2. \quad (59)$$

VI. NUMERICAL CALCULATIONS

In our previous article [3] we justified using the quarkonium–nucleus $q\bar{q}A$ scattering as a model of pA collisions. It also serves as the QCD ingredient for the deep inelastic eA scattering. Therefore, we extend the use of this model in this section for the incoherent diffraction.

We fix the quarkonium size at $r=0.2$ fm. Dependence of all cross sections on r has been discussed at length in Refs. [1–3] where the interested reader is readily referred.

Because our main goal in this section is to illustrate the key features of the various diffraction channels, rather than giving a detailed quantitative analyses, we approximate the nuclear profile by the step function (cylindrical nucleus).

It is clear from the discussion in the previous section that to calculate the diffractive cross sections we need only to specify the dipole-nucleus scattering amplitude $N_A(\mathbf{r}, \mathbf{b}, y)$ and the dipole density $n_p(\mathbf{r}, \mathbf{r}', y)$. The dipole-proton scattering amplitude $N_p(\mathbf{r}, \mathbf{b}, y)$ is obtained from $N_A(\mathbf{r}, \mathbf{b}, y)$ in the limit $A \to 1$.

For the forward elastic dipole-nucleus scattering amplitude $N_A(\mathbf{r}, \mathbf{b}, y)$ we use the KKT model [46], which is based on analytical analysis in Ref. [47]. It successfully describes the inclusive hadron production in the RHIC kinematic region (at the central and forward rapidities).

For the dipole density we use the leading BFKL solution in the diffusion approximation:

$$n_p(r, r', Y - y) = \frac{1}{2\pi^2}\frac{1}{rr'}\sqrt{\frac{\pi}{14\zeta(3)\bar{\alpha}_s\, d(Y-y)}} \times e^{(\alpha_P - 1)(Y-y)} e^{-\frac{\ln^2 \frac{r}{r'}}{14\zeta(3)\bar{\alpha}_s d(Y-y)}}. \quad (60)$$

Parameter d is equal to unity in the leading-order (LO) BFKL. To obtain the hadron diffractive cross section we convoluted the gluon cross sections (49) and (51) with the LO pion fragmentation function given in Ref. [48].

A convenient way to study the nuclear dependence of particle production is to consider the nuclear modification factor defined as follows

$$R^{pA}_{\rm diff}(k_T, y) = \frac{\frac{d\sigma^{pA}_{\rm diff}(k_T, y)}{d^2k_T dy}}{A\,\frac{d\sigma^{pp}_{\rm diff}(k_T, y)}{d^2k_T dy}}. \quad (61)$$

We calculate the diffractive gluon production in pp collisions, which is required as a baseline for the calculation of the nuclear modification factor (61), by setting $A = 1$ in the formula for the corresponding cross section in pA collisions. The nuclear modification factor is defined in such a way that a completely incoherent *scattering* would yield $R^{pA}_{\rm diff}(k_T, y) = 1$. The results of the calculations are exhibited in Fig. 1

We see that the nuclear modification factor is rapidly decreasing with rapidity for the coherent diffraction case and is almost independent of rapidity for the incoherent case. This trend continues even at the forward LHC energies [3]. In contrast to inclusive hadron production that saturates already in the forward rapidities at RHIC [46,49], we expect that the coherent diffraction cross section saturates at much higher energies and rapidities, perhaps at the forward rapidities at LHC (see Ref. [3] for an extensive discussion). As Fig. 1 implies, the incoherent diffractive gluon production is saturated already in the central rapidity region at RHIC.

We observe in Fig. 1 a parametric enhancement by a factor $\sim A^{1/3}$ of the coherent diffractive cross section with respect to the incoherent one. This is a benchmark of the classical gluon field of the nucleus in which quantum fluctuations are suppressed by $A^{1/3}$. This feature is also seen in Fig. 2 where we show the ratio of the cross sections for coherent and incoherent diffractive gluon production for pA collisions at different energies. To illustrate the atomic number dependence of this ratio we show three cases: $A = 200$, $A = 100$, and $A = 20$.

In Fig. 2 we can see that the fraction of the incoherent diffractive events increases from RHIC to LHC. This happens because the gluon saturation effects in proton are still not strong enough to unitarize the cross section. Remember, this allowed us to expand the scattering amplitude as shown in Eq. (38). Our estimate [Eq. (40)] shows that this approximation is valid for about six units of rapidity starting from the rapidity $y_1 \simeq 1$ at RHIC. Therefore, our conclusion that the fraction of incoherent diffractive events increases holds up to the rapidity $y_2 \simeq 3$ at the LHC. As soon as the gluon distribution of the incident proton saturates, the incoherent diffraction cross section vanishes, as can be seen in Eq. (20). This effect, however, is not included in our present model.

Finally, it may be challenging to experimentally distinguish the coherent and incoherent diffractive cross sections. In part it is related to the difficulty of performing measurements at very forward angles. One usually measures an event with large rapidity gap between the produced hadronic system and the target remnants in the forward direction (that may or may not be an intact nucleus). In such a likely case we consider the nuclear modification factor for a sum of coherent and incoherent diffractive channels. The result is

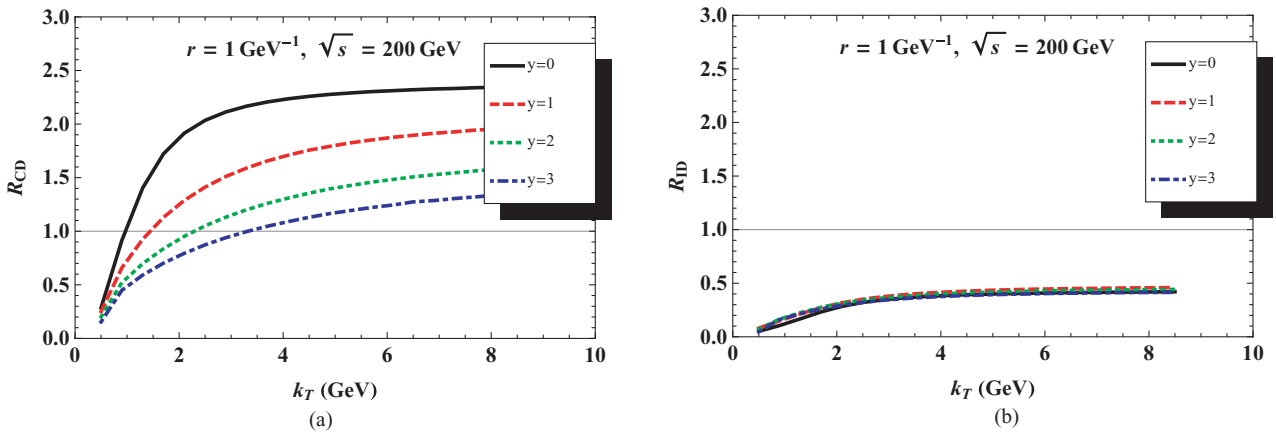

FIG. 1. (Color online) Nuclear modification factor for (a) coherent diffraction and (b) incoherent diffraction for RHIC at different rapidities.

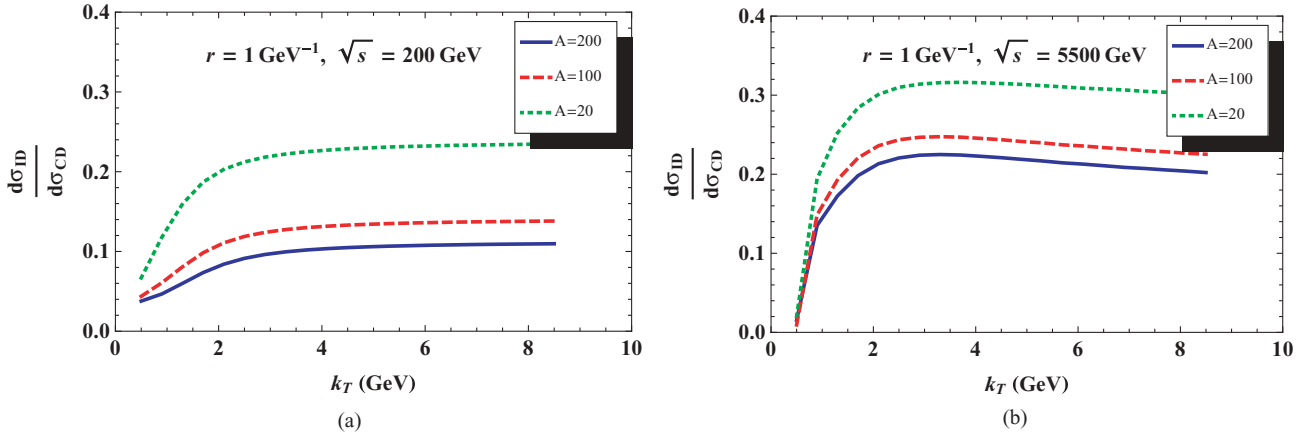

FIG. 2. (Color online) Ratio of the cross sections for coherent and incoherent diffractive gluon production in pA collisions at midrapidity: (a) RHIC and (b) LHC. (Solid blue line) $A = 200$. (Dashed red line) $A = 100$. (Dotted green line) $A = 20$.

displayed in Fig. 3. We can see that the predictions for the total diffractive cross section are similar to those of the inclusive hadron production [49]. Therefore, it is very important to experimentally separate contributions of coherent and incoherent diffraction. The former is especially useful for studying the low x QCD due to its strong and nontrivial energy, rapidity, and atomic number dependence.

Let us also mention that electromagnetic interactions also contribute to diffraction processes in pA collisions. If they become large, as argued in Ref. [50], it may present an additional experimental challenge. We intend to analyze contribution of the electromagnetic interactions in a separate publication.

To conclude this section, we emphasize that Figs. 1, 2, and 3 are an *illustration* of general features expected in various diffractive channels. As we have mentioned more than once in this article, application of realistic experimental cuts, which are unique for every experiment, will significantly change the absolute values of the cross sections and relative importance of the coherent and the incoherent channels. A dedicated study is required in each case, although the key features displayed in Figs. 1, 2, and 3 will perhaps remain unchanged.

VII. SUMMARY

To summarize, we calculated the cross section for the incoherent diffractive gluon production in $q\bar{q}A$ collisions, which is a prototype of pA collisions at RHIC and LHC and γ^*A ones at EIC. We took into account the gluon saturation, i.e., color glass condensate, effects. We then compared prediction of diffractive hadron production in coherent (calculated previously in Ref. [1–3]) and incoherent diffraction.

Coherent diffractive gluon production has a very characteristic energy, rapidity, and atomic number dependence that makes it a powerful tool for studying the leading mean-field contribution to the color glass condensate. Incoherent diffraction arises from contributions to the gluon field correlations beyond the mean-field approximation. Its experimental study can reveal the dynamics of quantum fluctuations in the CGC. Unlike the nuclear modification factor for coherent diffractive gluon production the nuclear modification factor for incoherent diffraction is not expected to exhibit a significant rapidity and energy dependence. Ratio of the coherent and incoherent inclusive diffractive cross sections is predicted to increase from RHIC to LHC *if* the gluon saturation effects in proton

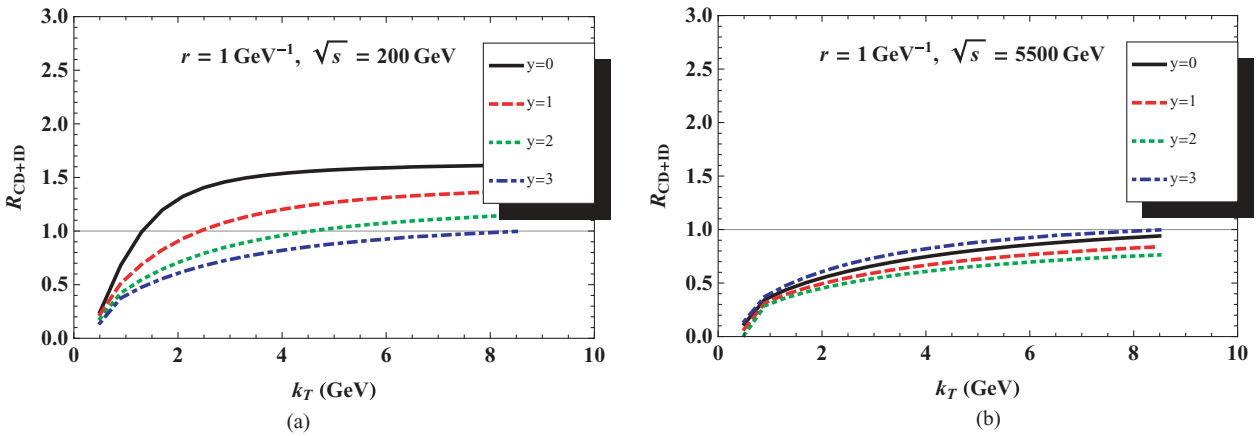

FIG. 3. (Color online) Nuclear modification factor for the sum of coherent and incoherent diffractive cross sections for (a) RHIC and (b) LHC at different rapidities.

are small. Otherwise, the ratio will decrease approaching the unitarity limit (i.e., zero).

Finally, one may consider measuring a diffractive event with large rapidity gap but without distinguishing contributions of coherent and incoherent components. Although in this case many interesting features of coherent and incoherent channels get averaged out, the corresponding cross section as well as the nuclear modification factor are expected to display a nontrivial behavior as a function of energy, atomic number, and transverse momentum. This behavior is sensitive to the underlying parton dynamics and thus can serve as a discriminator of different models. We are certain that studying diffraction at RHIC, LHC, and EIC can become an important tool in accessing the detailed structure of QCD at low x.

ACKNOWLEDGMENTS

I thank Dima Kharzeev, Yura Kovchegov, and J.-W. Qiu for informative discussions. I am grateful to Wlodek Guryn for encouragement and for explaining to me numerous experimental challenges in measurements of diffractive processes at RHIC. This work was supported in part by the US Department of Energy under Grant No. DE-FG02-87ER40371. I thank RIKEN, BNL, and the U.S. Department of Energy (Contract No. DE-AC02-98CH10886) for providing facilities essential for the completion of this work.

APPENDIX

In this Appendix we derive Eq. (37). For notation simplicity we replace the coordinates $\mathbf{x}$, $\mathbf{y}$, $\mathbf{z}_\sigma$ in the scattering amplitudes by subscript σ, with $\sigma = 1, 2$. We have

$$\sum_{f\neq i}\langle A_f|\Gamma_1^{q\bar{q}GA}(s,\mathbf{B},\{\mathbf{b}_a\})|A_i\rangle^\dagger\langle A_f|\Gamma_2^{q\bar{q}GA}(s,\mathbf{B},\{\mathbf{b}_a\})|A_i\rangle$$
$$=\langle A_i|\Gamma_1^{q\bar{q}GA}(s,\mathbf{B},\{\mathbf{b}_a\})\,\Gamma_2^{q\bar{q}GA}(s,\mathbf{B},\{\mathbf{b}_a\})|A_i\rangle - \langle A_i|\Gamma_1^{q\bar{q}GA}(s,\mathbf{B},\{\mathbf{b}_a\})|A_i\rangle\langle A_i|\Gamma_2^{q\bar{q}GA}(s,\mathbf{B},\{\mathbf{b}_a\})|A_i\rangle, \tag{A1}$$

Similarly to Eq. (18) we write

$$\Gamma_1^{q\bar{q}GA}(s,\mathbf{B},\{\mathbf{b}_a\})\,\Gamma_2^{q\bar{q}GA}(s,\mathbf{B},\{\mathbf{b}_a\}) = 1-\prod_{a=1}^{A}\left[1-\Gamma_1^{q\bar{q}GN}(s,\mathbf{B}-\mathbf{b}_a)\right] - \prod_{a=1}^{A}\left[1-\Gamma_2^{q\bar{q}GN}(s,\mathbf{B}-\mathbf{b}_a)\right] + \prod_{a=1}^{A}\left[1-\Gamma_1^{q\bar{q}GN}(s,\mathbf{B}-\mathbf{b}_a)\right]\left[1-\Gamma_2^{q\bar{q}GN}(s,\mathbf{B}-\mathbf{b}_a)\right] \tag{A2}$$

Averaging over the nucleus

$$\langle A_i|\Gamma_1^{q\bar{q}GA}(s,\mathbf{B},\{\mathbf{b}_a\})\,\Gamma_2^{q\bar{q}GA}(s,\mathbf{B},\{\mathbf{b}_a\})|A_i\rangle = 1-e^{-\int d^2b\Gamma_1^{q\bar{q}GN}(s,\mathbf{B}-\mathbf{b})\rho T_A(b)} - e^{-\int d^2b\Gamma_2^{q\bar{q}GN}(s,\mathbf{B}-\mathbf{b})\rho T_A(b)} + e^{-\int d^2b[\Gamma_1^{q\bar{q}GN}(s,\mathbf{B}-\mathbf{b})+\Gamma_2^{q\bar{q}GN}(s,\mathbf{B}-\mathbf{b})-\Gamma_1^{q\bar{q}GN}(s,\mathbf{B}-\mathbf{b})\Gamma_2^{q\bar{q}GN}(s,\mathbf{B}-\mathbf{b})]\rho T_A(b)} \tag{A3}$$

and subtracting the coherent part

$$\left[1-\Gamma_1^{q\bar{q}GA}(s,\mathbf{B},\{\mathbf{b}_a\})\right]\left[1-\Gamma_2^{q\bar{q}GA}(s,\mathbf{B},\{\mathbf{b}_a\})\right] \tag{A4}$$

we obtain

$$\sum_{f\neq i}\langle A_f|\Gamma_1^{q\bar{q}GA}(s,\mathbf{B},\{\mathbf{b}_a\})|A_i\rangle^\dagger\langle A_f|\Gamma_2^{q\bar{q}GA}(s,\mathbf{B},\{\mathbf{b}_a\})|A_i\rangle$$
$$= e^{-\int d^2b[\Gamma_1^{q\bar{q}GN}(s,\mathbf{B}-\mathbf{b})+\Gamma_2^{q\bar{q}GN}(s,\mathbf{B}-\mathbf{b})-\Gamma_1^{q\bar{q}GN}(s,\mathbf{B}-\mathbf{b})\Gamma_2^{q\bar{q}GN}(s,\mathbf{B}-\mathbf{b})]\rho T_A(b)} - e^{-\int d^2b[\Gamma_1^{q\bar{q}GN}(s,\mathbf{B}-\mathbf{b})+\Gamma_2^{q\bar{q}GN}(s,\mathbf{B}-\mathbf{b})]\rho T_A(b)} \tag{A5}$$
$$= e^{-\int d^2b[\Gamma_1^{q\bar{q}GN}(s,\mathbf{B}-\mathbf{b})+\Gamma_2^{q\bar{q}GN}(s,\mathbf{B}-\mathbf{b})-\Gamma_1^{q\bar{q}GN}(s,\mathbf{B}-\mathbf{b})\Gamma_2^{q\bar{q}GN}(s,\mathbf{B}-\mathbf{b})]\rho T_A(b)} \times\left\{1-e^{-\int d^2b\Gamma_1^{q\bar{q}GN}(s,\mathbf{B}-\mathbf{b})\Gamma_2^{q\bar{q}GN}(s,\mathbf{B}-\mathbf{b})\rho T_A(b)}\right\} \tag{A6}$$
$$= e^{-\frac{1}{2}[\sigma_{\rm tot}^{q\bar{q}GN}(s,1)+\sigma_{\rm tot}^{q\bar{q}GN}(s,2)-\frac{1}{4\pi R_p^2}\sigma_{\rm tot}^{q\bar{q}GN}(s,1)\,\sigma_{\rm tot}^{q\bar{q}GN}(s,2)]\,\rho T_A(\mathbf{b})} \times\left\{1-e^{-\frac{1}{2}\frac{1}{4\pi R_p^2}\sigma_{\rm tot}^{q\bar{q}GN}(s,1)\,\sigma_{\rm tot}^{q\bar{q}GN}(s,2)\,\rho T_A(\mathbf{b})}\right\}, \tag{A7}$$

as advertised. In the last line we employed the approximation $R_p \ll R_A$ that allows us to write using an analog of Eq. (12):

$$\int d^2b\Gamma_1^{q\bar{q}GN}(s,\mathbf{B}-\mathbf{b})\Gamma_2^{q\bar{q}GN}(s,\mathbf{B}-\mathbf{b})\,\rho T_A(b) = \frac{1}{4}\sigma_{\rm tot}^{q\bar{q}GA}(s,1)\,\sigma_{\rm tot}^{q\bar{q}GA}(s,2)\int d^2b\frac{1}{\left(\pi R_p^2\right)^2}e^{-2\frac{(\mathbf{b}-\mathbf{B})^2}{R_p^2}}\,\rho T_A(b)$$
$$\approx \frac{1}{4}\sigma_{\rm tot}^{q\bar{q}GA}(s,1)\,\sigma_{\rm tot}^{q\bar{q}GA}(s,2)\,\frac{1}{\left(\pi R_p^2\right)^2}\,\rho T_A(\mathbf{B})\int d^2b' e^{-2\frac{b'^2}{R_p^2}}$$
$$= \frac{1}{4}\sigma_{\rm tot}^{q\bar{q}GA}(s,1)\,\sigma_{\rm tot}^{q\bar{q}GA}(s,2)\,\frac{1}{2\pi R_p^2}\,\rho T_A(\mathbf{B}). \tag{A8}$$

where $\mathbf{b}' = \mathbf{b} - \mathbf{B}$ and $\mathbf{b}'^2 \ll \mathbf{b}^2, \mathbf{B}^2$.

[1] Y. Li and K. Tuchin, Phys. Rev. D **77**, 114012 (2008).
[2] Y. Li and K. Tuchin, Nucl. Phys. **A807**, 190 (2008).
[3] Y. Li and K. Tuchin, Phys. Rev. C **78**, 024905 (2008).
[4] L. V. Gribov, E. M. Levin, and M. G. Ryskin, Phys. Rep. **100**, 1 (1983).
[5] A. H. Mueller and J. W. Qiu, Nucl. Phys. **B268**, 427 (1986).
[6] L. D. McLerran and R. Venugopalan, Phys. Rev. D **49**, 2233 (1994); **49**, 3352 (1994); **50**, 2225 (1994).
[7] Y. V. Kovchegov, Phys. Rev. D **54**, 5463 (1996); **55**, 5445 (1997).
[8] I. Balitsky, Nucl. Phys. **B463**, 99 (1996); Phys. Rev. Lett. **81**, 2024 (1998); Phys. Rev. D **60**, 014020 (1999).

[9] J. Jalilian-Marian, A. Kovner, A. Leonidov, and H. Weigert, Nucl. Phys. **B504**, 415 (1997); Phys. Rev. D **59**, 014014 (1998).
[10] J. Jalilian-Marian, A. Kovner, and H. Weigert, Phys. Rev. D **59**, 014015 (1998).
[11] A. Kovner, J. G. Milhano, and H. Weigert, Phys. Rev. D **62**, 114005 (2000); H. Weigert, Nucl. Phys. **A703**, 823 (2002).
[12] E. Iancu, A. Leonidov, and L. D. McLerran, Nucl. Phys. **A692**, 583 (2001).
[13] E. Ferreiro, E. Iancu, A. Leonidov, and L. McLerran, Nucl. Phys. **A703**, 489 (2002).
[14] Y. V. Kovchegov, Phys. Rev. D **60**, 034008 (1999).
[15] R. J. Glauber, Phys. Rev. **100**, 242 (1955).
[16] A. Kovner and M. Lublinsky, Phys. Rev. Lett. **94**, 181603 (2005); Phys. Rev. D **71**, 085004 (2005).
[17] A. Kovner, M. Lublinsky, and U. Wiedemann, J. High Energy Phys. 06 (2007) 075.
[18] E. Iancu and D. N. Triantafyllopoulos, Nucl. Phys. **A756**, 419 (2005).
[19] E. Iancu, A. H. Mueller, and S. Munier, Phys. Lett. **B606**, 342 (2005).
[20] J. Bartels *et al.*, DESY-PROC-2007-02 (2007), p. 549.
[21] A. H. Mueller, Nucl. Phys. **B415**, 373 (1994); A. H. Mueller and B. Patel, *ibid.* **B425**, 471 (1994); A. H. Mueller, *ibid.* **B437**, 107 (1995).
[22] M. Wusthoff, Phys. Rev. D **56**, 4311 (1997).
[23] J. Bartels, H. Jung, and M. Wusthoff, Eur. Phys. J. C **11**, 111 (1999).
[24] B. Z. Kopeliovich, A. Schafer, and A. V. Tarasov, Phys. Rev. D **62**, 054022 (2000).
[25] Y. V. Kovchegov, Phys. Rev. D **64**, 114016 (2001) [Erratum-*ibid.* **68**, 039901 (2003)].
[26] K. J. Golec-Biernat and C. Marquet, Phys. Rev. D **71**, 114005 (2005).
[27] C. Marquet, Nucl. Phys. **B705**, 319 (2005).
[28] C. Marquet, Phys. Rev. D **76**, 094017 (2007).
[29] S. Munier and A. Shoshi, Phys. Rev. D **69**, 074022 (2004).
[30] H. Kowalski, T. Lappi, C. Marquet, and R. Venugopalan, Phys. Rev. C **78**, 045201 (2008).
[31] L. Frankfurt, V. Guzey, and M. Strikman, Phys. Rev. D **71**, 054001 (2005); Phys. Lett. **B586**, 41 (2004).
[32] V. Guzey and M. Strikman, Phys. Rev. C **75**, 045208 (2007).
[33] A. H. Mueller, Nucl. Phys. **B335**, 115 (1990).
[34] E. Avsar, G. Gustafson, and L. Lonnblad, J. High Energy Phys. 07 (2005) 062; 01 (2007) 012; 12 (2007) 012.
[35] B. Z. Kopeliovich, I. K. Potashnikova, and I. Schmidt, Phys. Rev. C **73**, 034901 (2006).
[36] A. B. Kaidalov, V. A. Khoze, A. D. Martin, and M. G. Ryskin, Acta Phys. Pol. B **34**, 3163 (2003).
[37] V. Guzey and M. Strikman, Phys. Lett. **B633**, 245 (2006) [Erratum-*ibid.* **B663**, 456 (2008)].
[38] A. Kovner, M. Lublinsky, and H. Weigert, Phys. Rev. D **74**, 114023 (2006).
[39] A. Kovner and U. A. Wiedemann, Phys. Rev. D **64**, 114002 (2001).
[40] B. Z. Kopeliovich, A. Schafer, and A. V. Tarasov, Phys. Rev. C **59**, 1609 (1999).
[41] K. Tuchin, Phys. Lett. **B593**, 66 (2004).
[42] E. Levin and K. Tuchin, Nucl. Phys. **B573**, 833 (2000).
[43] Y. V. Kovchegov and K. Tuchin, Phys. Rev. D **65**, 074026 (2002).
[44] E. A. Kuraev, L. N. Lipatov, and V. S. Fadin, Sov. Phys. JETP **45**, 199 (1977) [Zh. Eksp. Teor. Fiz. **72**, 377 (1977)].
[45] I. I. Balitsky and L. N. Lipatov, Sov. J. Nucl. Phys. **28**, 822 (1978) [Yad. Fiz. **28**, 1597 (1978)].
[46] D. Kharzeev, Y. V. Kovchegov, and K. Tuchin, Phys. Lett. **B599**, 23 (2004).
[47] D. Kharzeev, Y. V. Kovchegov, and K. Tuchin, Phys. Rev. D **68**, 094013 (2003).
[48] B. A. Kniehl, G. Kramer, and B. Potter, Nucl. Phys. **B597**, 337 (2001).
[49] K. Tuchin, Nucl. Phys. **A798**, 61 (2008).
[50] V. Guzey and M. Strikman, Phys. Rev. C **77**, 067901 (2008).